



**Evaluating the UEB  
snow model in the  
Noah Land-Surface  
Model**

R. Sultana et al.

This discussion paper is/has been under review for the journal Hydrology and Earth System Sciences (HESS). Please refer to the corresponding final paper in HESS if available.

# Evaluating the Utah Energy Balance's (UEB) snow model in the Noah Land-Surface Model

R. Sultana<sup>1,2</sup>, K.-L. Hsu<sup>2</sup>, J. Li<sup>2</sup>, and S. Sorooshian<sup>2</sup>

<sup>1</sup>California State University, Long Beach, CA, USA

<sup>2</sup>University of California, Irvine, CA, USA

Received: 5 September 2013 – Accepted: 13 October 2013 – Published: 7 November 2013

Correspondence to: R. Sultana (rebeka.sultana@csulb.edu) and K.-L. Hsu (kuolinh@uci.edu)

Published by Copernicus Publications on behalf of the European Geosciences Union.

Title Page

Abstract

Introduction

Conclusions

References

Tables

Figures



Back

Close

Full Screen / Esc

Printer-friendly Version

Interactive Discussion







## Evaluating the UEB snow model in the Noah Land-Surface Model

R. Sultana et al.

[Title Page](#)

[Abstract](#)

[Introduction](#)

[Conclusions](#)

[References](#)

[Tables](#)

[Figures](#)

[⏪](#)

[⏩](#)

[◀](#)

[▶](#)

[Back](#)

[Close](#)

[Full Screen / Esc](#)

[Printer-friendly Version](#)

[Interactive Discussion](#)

Niu et al. (2011) replaced Noah's single-layer snowpack with multiple layers to explicitly capture the non-linear temperature gradient of the snowpack. Complex snow models (ex, SNTHERM, Jordan, 1991; CLM, Dai, 2003; SAST, Jin et al., 1999b) also apply finite-difference models to simulate snowpack temperatures. In these finite-difference models, changes in snow properties within layers (Anderson, 1976; Colbeck, 1982; Jordan, 1991; Arons and Colbeck, 1995) are estimated, which are useful in some applications. However, the only piece of information required for climate study and hydrologic prediction is the snow-skin temperature, because the temperature gradient between the snow surface and atmosphere drives the turbulent fluxes (Luce and Tarboton, 2001).

In this study, we address the problem of Noah's SWE bias and early snowmelt by implementing the snow-surface temperatures and snow-melt processes of the Utah Energy Balance (UEB) model in the Noah LSM (Tarboton et al., 1994; Tarboton, 1994; Tarboton and Luce, 1996; Luce and Tarboton, 2001). Similar to the Noah model, UEB simulates snowpack as a single layer but applies the force-restore method, which, unlike the finite-difference methods, implicitly represents temperature profiles within the snowpack.

The force-restore method has also been assessed by Dickinson et al. (2003) for snow-surface temperature prediction, but it has been applied more widely in various land-surface and hydrologic models to estimate soil temperature (Deardorff, 1978; Noilhand and Planton, 1989; Mahfouf et al., 1995; Dickinson, 1993; Sellers et al., 1996; Dai et al., 2003; Kahan et al., 2006; Gao et al., 2008). The method has been popular because it uses a minimum number of prognostic variables while capturing important physical processes with reasonable computational efficiency (Ren and Xue, 2004). Previous studies indicate that this method underestimates the temperatures of the deep layer, even with some modifications (e.g., Mahfouf et al., 1995; Ren and Xue, 2004; Luce and Tarboton, 2001; You, 2004; Luce and Tarboton, 2010). In this study, we have chosen the force-restore-based UEB snow model as the target in the Noah LSM for benefiting from its effectiveness in snow-surface temperature estimation, while keeping the Noah land-surface model's snow submodel as a single layer model. Single-layer

## Evaluating the UEB snow model in the Noah Land-Surface Model

R. Sultana et al.

Title Page

Abstract

Introduction

Conclusions

References

Tables

Figures

⏪

⏩

◀

▶

Back

Close

Full Screen / Esc

Printer-friendly Version

Interactive Discussion

snow models like Noah LSM are less complex to apply as it requires a small number of input variables but still can retain important information about the processes, which are advantageous in applying these models in global climate models (GCMs) or regional climate models (RCMs) (e.g. Dickinson, 1993). In addition, the UEB model applies the force-restore method along with evaluating the internal energy of the snowpack, which is used consecutively to determine the snow-melt events by retaining liquid water within the snowpack (Tarboton et al., 1994; Tarboton, 1994; Tarboton and Luce, 1996; Luce and Tarboton, 2001).

Noah's current approach for simulating snow temperature and snow-melt conditions will be described in the next subsection. The UEB snow model is discussed in Sect. 3. In Sect. 4, the study areas and forcing information are given. Results and discussion on the modified Noah model are given in Sect. 5. Finally, the conclusions are drawn in Sect. 6.

## 2 Current formulation and enhancement

### 2.1 Current method for snow-temperature estimation

In the Noah LSM, snow-surface temperature ( $T_s$ ) for the entire snowpack is estimated in a two-step process and Fig. 2 is the graphical representation of the both computation processes during a snow season. In the first step, energy balance between the snowpack and the overlying air and underlying top soil an intermediate temperature ( $T_{12}$ ) is estimated (Koren et al., 1999; Ek et al., 2003). Detail of the energy balance equation is given in the Appendix A. The method allows this temperature to rise above freezing temperature ( $T_{\text{freeze}}$ ) even when the model grid is 100 % covered with snow as can be seen in Fig. 2b.

In the second step, the effective temperature for a model grid ( $T_1$ ) is adjusted by accounting for the fractional snow cover ( $f_{sca}$ ) in the ground as (Koren et al., 1999):

$$T_1 = T_{12}, \quad (T_{12} \leq T_{freeze}) \quad (1a)$$

$$T_1 = T_{freeze} \cdot f_{sca}^2 + T_{12}(1 - f_{sca}^2), \quad (T_{12} > T_{freeze}). \quad (1b)$$

Equation (1) describes that, when the ground is completely snow-covered,  $T_1$  is essentially snow surface temperature which can be below or at freezing temperature. On the other hand,  $T_1$  can be above freezing temperature when the ground is partially covered with snow. The one of primary deficiency of the control model is that the snow sub model is conditioned to initiate snowmelt whenever the temperature  $T_1$  is at or above the freezing point (Fig. 2d). But, snow surface at freezing point is not the single factor to cause snowmelt. Snowmelt initiates only after the entire snowpack is isothermal at 0°C which is called as warming phase (Dingman, 2009). This phase is followed by a ripening phase when melt water can retain in the snowpack until it exceeds liquid water holding capacity of the snowpack. Therefore, to initiate snowmelt, it is crucial to know at which state the snowpack is which can be determined by accounting for the internal energy of the snowpack (Tarboton et al., 1996). Further, the warming and ripening processes are not considered in Noah's snow sub-model and, therefore, the model overestimates the net energy which is used to control snow-melt outflow rate (Livneh et al., 2009; Lundquist and Flint, 2006) resulting in a faster melt rate.

## 2.2 The UEB snow model

To overcome the deficiencies in Noah's snow model, snow-surface temperature and snow-melt processes of the Utah Energy Balance (UEB) snow model are evaluated as an alternate method to the existing snow model. The UEB model was originally developed by Tarboton et al. (1994) and Tarboton and Luce (1996), and later efforts have been made to improve the model performance (Luce and Tarboton, 2001, 2010; You, 2004). A detailed discussion of the UEB model and the force-restore method can

### Evaluating the UEB snow model in the Noah Land-Surface Model

R. Sultana et al.

Title Page

Abstract

Introduction

Conclusions

References

Tables

Figures

⏪

⏩

◀

▶

Back

Close

Full Screen / Esc

Printer-friendly Version

Interactive Discussion



be found in Tarboton et al. (1994, 1995), Tarboton and Luce (1996), and Luce and Tarboton (2001), while a brief discussion of the model's physical processes pertinent to this paper is given below.

## 2.2.1 Snow surface temperature formulation

To compute snow surface temperature UEB model applies energy balance at the snow surface unlike Noah LSM where net energy for the entire snowpack layer is computed. In reality, the snow surface temperature is cooler (warmer) than the entire snowpack temperature at night (day) time and therefore results a non-linear temperature gradient within a snowpack layer. The UEB model approximates this temperature gradient by differentiating surface temperature ( $T_s$ ) from the average snowpack temperature ( $\bar{T}$ ). At every time step, snow-skin temperature ( $T_s$ ) is numerically solved using the Newton–Raphson method by employing the following (Tarboton and Luce, 1996):

$$Q_{cs}(T_s, \bar{T}) = Q_{\text{forcing}}(T_s) \quad (2a)$$

$$Q_{\text{forcing}}(T_s) = Q_{\text{snet}} + Q_{\text{lin}} - Q_{\text{l,out}}(T_s) + Q_{\text{h}}(T_s) + Q_{\text{le}}(T_s) + Q_{\text{p}} \quad (2b)$$

where  $Q_{cs}$  is the heat flux because of the temperature gradient within the snowpack and  $Q_{\text{forcing}}$  is essentially the heat flux considering all of the energy components at the snow surface,  $Q_{\text{snet}}$  is the net short-wave energy,  $Q_{\text{lin}}$  is the incoming long-wave radiation,  $Q_{\text{l,out}}$  is the outgoing long-wave radiation from the snowpack,  $Q_{\text{h}}$  is the sensible heat flux to/from the snow,  $Q_{\text{le}}$  is the latent heat flux to/from the snow, and  $Q_{\text{p}}$  is the energy advected by precipitation into the snow. The turbulent heat fluxes ( $Q_{\text{h}}$  and  $Q_{\text{le}}$ ) and the outgoing radiative flux ( $Q_{\text{l,out}}$ ) are functionally dependent on the surface temperature  $T_s$  (Tarboton and Luce, 1996; You, 2004). Physically snow temperature cannot be greater than  $0^\circ\text{C}$  and, thus, the upper bound of  $T_s$  is constrained to freezing temperature.

## Evaluating the UEB snow model in the Noah Land-Surface Model

R. Sultana et al.

Title Page

Abstract

Introduction

Conclusions

References

Tables

Figures

⏪

⏩

◀

▶

Back

Close

Full Screen / Esc

Printer-friendly Version

Interactive Discussion



$Q_{cs}$  in Eq. (2a) is derived from thermal-diffusion equation which describes how temperature changes with time along the depth of a layer and the equation is (Luce and Tarboton, 2001, 2010; You, 2004):

$$\frac{\partial T}{\partial t} = \left(\frac{\lambda}{c}\right) \frac{\partial^2 T}{\partial z^2} = k \frac{\partial^2 T}{\partial z^2} \quad (3)$$

with the boundary condition for temperature as:

$$T|_{z=0} = \bar{T} + A \sin \omega t, \quad (4)$$

where  $T$  is the temperature,  $t$  is time,  $z$  is the depth measured downward from the surface,  $c$  is the volumetric heat capacity, and  $\lambda$  is the heat conductivity,  $k$  is the thermal diffusivity of snow ( $= \frac{c}{\lambda}$ ),  $\bar{T}$  is the mean snow-surface temperature,  $A$  is the amplitude of the diurnal snow-temperature wave at the surface, and  $\omega$  is the angular velocity of the Earth's rotation (i.e.,  $\omega = 2\pi/24 \text{ rad h}^{-1}$ ). An approximate solution of Eq. (4) for sinusoidal temperature fluctuation is (Carslaw and Jaeger, 1959):

$$T(z, t) = \bar{T} + A e^{-\frac{z}{d}} \sin\left(\omega t - \frac{z}{d}\right) \quad (5)$$

where  $d$  is the diurnal damping depth, and  $d = \sqrt{2k/\omega}$ . The equation may be used to calculate the temperature gradient with depth which can be used with the heat conductivity ( $\lambda$ ) to compute heat flux ( $Q_c$ ) (Lin, 1980; Hu and Islam, 1995; Luce and Tarboton, 2001; Gao et al., 2008):

$$Q_c(z, t) = \lambda \frac{\partial T(z, t)}{\partial z} = \frac{\lambda}{d} \left[ A e^{-\frac{z}{d}} \sin(\omega t - z/d) + A e^{-\frac{z}{d}} \cos(\omega t - z/d) \right]. \quad (6)$$

Further, rearranging Eq. (5) and then differentiating with respect to time  $t$ :

$$A e^{(-z/d)} \sin(\omega t - z/d) = T(z, t) - \bar{T} \quad (7a)$$

$$A e^{(-z/d)} \cos(\omega t - z/d) = \frac{1}{\omega} \frac{\partial T(z, t)}{\partial t}. \quad (7b)$$

**Evaluating the UEB snow model in the Noah Land-Surface Model**

R. Sultana et al.

Discussion Paper | Discussion Paper | Discussion Paper | Discussion Paper | Discussion Paper

Title Page	
Abstract	Introduction
Conclusions	References
Tables	Figures
⏪	⏩
◀	▶
Back	Close
Full Screen / Esc	
Printer-friendly Version	
Interactive Discussion	



Using Eqs. (7a) and (7b), Eq. (6) can be written as:

$$Q_c(z, t) = \frac{\lambda}{d} \left( \frac{1}{\omega} \frac{\partial T(z, t)}{\partial t} + T(z, t) - \bar{T} \right). \quad (8a)$$

At the surface boundary where  $z = 0$ , the heat flux at the surface ( $Q_{cs}$ ) is:

$$Q_c(0, t) = Q_{cs} = \frac{\lambda}{d} \left( \frac{1}{\omega} \frac{\partial T(0, t)}{\partial t} + T(0, t) - \bar{T} \right) \quad (8b)$$

$$Q_{cs} = \frac{\lambda}{d} \left( \frac{1}{\omega} \frac{\partial T_s}{\partial t} + T_s - \bar{T} \right). \quad (8c)$$

Equation (8c) is the basis for the force-restore method and with the finite-difference approximation for  $\partial T_s / \partial t$  in Eq. (8c) results in:

$$Q_{cs} = \frac{\lambda}{d} \left( \frac{1}{\omega \Delta t} (T_s - T_{s_{lag1}}) + (T_s - \bar{T}) \right) \quad (9)$$

where  $\Delta t$  is the measurement time interval, and  $T_{s_{lag1}}$  is the surface temperature lagged by one time step, i.e., at  $t - \Delta t$ .

The average snow-surface temperature  $\bar{T}$  given in Eqs. (2)–(9) has not been defined consistently in the literature (see examples of various definitions of  $\bar{T}$  in Ren and Xue, 2004). In the UEB model,  $\bar{T}$  is defined as the depth-average snowpack temperature, which is derived from two state variables: snow water equivalent ( $W$ ) and internal energy ( $U$ ) of the snowpack. Internal energy  $U$  is defined as the energy to the melting point which means that, at  $0^\circ\text{C}$ , ice possesses zero heat content (Tarboton et al., 1994; Jin et al., 1999a, b). Not only snow temperature, internal energy has been also used as a prognostic variable by Lynch-Stieglitz (1994) and Jin et al. (1999b).

Snow temperature affects sublimation from the snow surface. UEB applies turbulent heat flux (Tarboton, 1994) while Noah LSM uses Penman equation (Wang et al., 2010) to compute sublimation.

## Evaluating the UEB snow model in the Noah Land-Surface Model

R. Sultana et al.

Title Page

Abstract

Introduction

Conclusions

References

Tables

Figures

⏪

⏩

◀

▶

Back

Close

Full Screen / Esc

Printer-friendly Version

Interactive Discussion



## 2.2.2 Snow-melt formulation

In UEB model, whenever internal energy is positive, the snowpack attains sufficient energy to initiate snow-melt and the snow-melt outflow rate  $M_r$  from ripened snow is simulated based on Male and Gray (1981) and is (Tarboton, 1994; Tarboton and Luce, 1996):

$$M_r = K_s S^3 \quad (10)$$

where  $S$  is the relative saturation in excess of the liquid water-holding capacity, and  $K_s$  is the snow-saturated hydraulic conductivity, which describes the water flux through the porous snowpack and is a function of snow density, porosity, and liquid water-holding capacity. The variation of  $K_s$  with a saturated water content of natural snow is not clear (Iida et al., 2000) and, hence,  $K_s$  is essentially a calibration parameter for each location (Tarboton and Luce, 1996). Different  $K_s$  values are reported in previous studies (Gray and Male, 1981; Tarboton and Luce, 1996; Zanotti et al., 2004; Mahat and Tarboton, 2011; Tarboton, 1994; You, 2004), but the model is not very sensitive to the value of  $K_s$ , and a  $K_s$  value of  $20 \text{ m h}^{-1}$  is used in this study, which reasonably describes the snow-melt rate and timing at the study sites.

The parameter  $S$  in Eq. (10) is derived from the following relationship:

$$S = \frac{\text{liquid water volume} - \text{capillary retention}}{\text{pore volume} - \text{capillary retention}} \quad (11)$$

where the value of variable  $S$  increases with increasing liquid water in the snowpack. Liquid water is the amount of water that can be retained in the snow pores against capillary forces, and consideration of capillary retention or liquid water-holding capacity can delay snowmelt during the ripening phase (Dingman, 2009). Amid the ripening phase, liquid water near the surface can refreeze with night-time cooling and thaw during day. This refreeze and thaw cycle can continue for days if the liquid water does not exceed the water-holding capacity of the snowpack. During the day, this cycle might

### Evaluating the UEB snow model in the Noah Land-Surface Model

R. Sultana et al.

Title Page

Abstract

Introduction

Conclusions

References

Tables

Figures

⏪

⏩

◀

▶

Back

Close

Full Screen / Esc

Printer-friendly Version

Interactive Discussion



need several hours to warm up and resume melting again (Dingman, 2009). Snow-melt starts once the liquid water in the snowpack exceeds the water-holding capacity, and the rate of melting increases with the increase of the amount of liquid water.

The parameter “liquid water-holding capacity” is difficult to measure from wet snow because, during the snow-melt metamorphism, snow can be supersaturated yet be below the liquid water-holding capacity due to the freeze-thaw cycle (Livneh et al., 2009). In various studies, the liquid water-holding capacity is quantified as 3–9 % of the volume of the snowpack (Denoth et al., 1984; Kattlemann, 1987; Kendra et al., 1994; Albert and Krajieski, 1998). Jordan (1991) used 4 % of the pore volume in SNTHERM, Lynch-Stieglitz (1994) used 5.5 % height of the compacted snow layer, while Dingman (2009) suggested 6 % of the pore space as the liquid water-holding capacity. Following Jordan (1991) and Denoth (2003), Livneh et al. (2009) applied 4 % of the pore volume of the liquid water-holding capacity in the Noah model. Because the density of the snowpack is different for fresh snow compared to old snow, Livneh et al. (2009) showed that 4 % of the pore volume can range from approximately 2.5 % of SWE depth for old snow to approximately 10 % of SWE depth for fresh snow. Here, we have used 5 % of the total mass of the snowpack (liquid and ice) as the liquid water- holding capacity (Tarboton et al., 1996), and the fraction of liquid water  $L_f$  is estimated as:

$$L_f = \frac{U}{\rho_w \lambda_f W} \quad (12)$$

where  $U$  is the internal energy of the snowpack,  $W$  is the snow-water equivalent,  $\rho_w$  is the density of water,  $\lambda_f$  is the heat of fusion of ice, and  $\rho_w \lambda_f W$  is the energy required to melt the entire snowpack at 0 °C. A sensitivity test of the liquid water-holding capacity is discussed in the conclusions section.

## HESSD

10, 13363–13406, 2013

### Evaluating the UEB snow model in the Noah Land-Surface Model

R. Sultana et al.

Title Page

Abstract

Introduction

Conclusions

References

Tables

Figures

⏪

⏩

◀

▶

Back

Close

Full Screen / Esc

Printer-friendly Version

Interactive Discussion

### 3 Application of the method

#### 3.1 Study area and input data

The Noah LSM requires seven input variables, and the forcing data from the North American Land Data Assimilation System (NLDAS-2) are used to drive the model. NLDAS forcing data are at  $1/8^\circ$ -grid resolution (approximately 12.5 km) and available at hourly time scale and discussed in detail by Cosgrove et al. (2003) and extensively validated by Luo et al. (2003) and Pinker et al. (2003). The model outputs are evaluated against ground-observation data at various SNOTEL stations located in the Sierra Nevada Mountains of California as well as at a SNOTEL site in Utah, which is close to a snow- surface temperature data collection site. Brief descriptions of these study areas are given below.

##### 3.1.1 SNOTEL stations in California

Snow-water equivalent (SWE) observations at SNOTEL sites in California are used here to verify the control and outputs of the modified models. These ground observations are at clear vegetated land and provide snow information with reasonable accuracy (Serreze et al., 1999). SNOTEL stations have also been used by others for Noah-related studies (Pan et al., 2003; Jin and Miller, 2007; Livneh et al., 2009; Barlage et al., 2010; Pederson et al., 2010). These stations measure daily SWE, 2 m air temperature, and precipitation, as well as soil moisture and soil-temperature data; a more comprehensive discussion about these sites is given on the Natural Resources Conservation Service (NRCS) website. Here, the data used are quality-controlled as described by Serreze et al. (1999), and a total of 22 SNOTEL stations have been used for the 7 yr period from June 2001–June 2008. The elevations of the Sierra Nevada Mountains stations range from 1576–2961 m.

Over the study period, the maximum SWE is observed at the highest-elevated station (SNOTEL Station #574) and was 2628 mm in 2006. This year was an El Niño year,

## Evaluating the UEB snow model in the Noah Land-Surface Model

R. Sultana et al.

[Title Page](#)

[Abstract](#)

[Introduction](#)

[Conclusions](#)

[References](#)

[Tables](#)

[Figures](#)

[⏪](#)

[⏩](#)

[◀](#)

[▶](#)

[Back](#)

[Close](#)

[Full Screen / Esc](#)

[Printer-friendly Version](#)

[Interactive Discussion](#)



which usually generates higher than normal SWEs in the Southwest (Jin and Miller, 2007).

Land-surface characteristics were derived from the grid cell within which SNOTEL stations are located. Although SNOTEL stations are at installed in open spaces, we wanted to simulate Noah with grid-scale attributes to facilitate model application at large scale. Detailed comparisons are shown for four Stations: #356, #508, #463, and #539, and elevation and average annual rainfall over these stations are given in Table 1. Later, an overview of the model performance over 21 stations is also provided.

### 3.1.2 T. W. Daniel Experimental Forest site, Utah

Utah State University (USU)'s T. W. Daniels Experimental Forest (TWDEF) has an experimental site (41.86° N, 111.50° W) at an elevation of 2600 m, roughly 30 km north-east of Logan along the border between Utah's Rich and Cache counties. Various properties of snow, vegetation, soil, and atmosphere are measured every 30 min at 12 monitoring weather stations and at an eddy covariance tower. Weather stations distributed across the site record air temperature, humidity, snow depth (when present), soil moisture, and sundry other quantities, while the eddy covariance system records atmospheric fluxes. However, snow-temperature data collection started from 2008; hence, for this work, water year 2009 data were used. More information about this study site can be found at <http://danielforest.usu.edu/Maps.aspx>.

Near the experimental site, a SNOTEL station (#1098) was also installed in July 2007, and the model was simulated using NLDAS grid data where the station resides. NLDAS precipitation data were bias-corrected using the daily precipitation data recorded at this station. Model-simulated snow-surface temperature and energy-flux data were verified using the TWDEF site records of snow-surface temperature and energy fluxes.

The location of the SNOTEL stations in California and Utah are shown in Fig. 1.

## HESSD

10, 13363–13406, 2013

### Evaluating the UEB snow model in the Noah Land-Surface Model

R. Sultana et al.

Title Page

Abstract

Introduction

Conclusions

References

Tables

Figures

⏪

⏩

◀

▶

Back

Close

Full Screen / Esc

Printer-friendly Version

Interactive Discussion



SWE is almost negligible, particularly at Station #463 (less than 20% of the ground observed maximum SWE).

The primary reason for the Noah land-surface model's negative bias in SWE estimation is because of imperfection in its current snow-physical processes, as discussed earlier. In addition, uncertainty in input can be quite substantial as well, especially in the mountainous environments. Precipitation, a primary input for quantifying snowfall, can be extremely variable in space and time in high-elevated areas. Mitchell et al. (2004) discussed this issue and pointed out that precipitation data in the NLDAS system are based on the National Weather Service (NWS) precipitation gauges. These gauges, located mostly in valleys, are known to underestimate higher-elevation precipitation (Pan et al., 2003). Pan et al. (2003) compared the NLDAS precipitation with SNOTEL precipitation from September 1996–September 1999 and found that SNOTEL precipitation is, on average, more than twice the amount of the NLDAS precipitation data. On the other hand, differences in other forcing data between NLDAS and those of stations were found to be insignificant (Luo et al., 2003).

Therefore, a simple precipitation bias-correction method was applied to NLDAS precipitation data, while no corrections were made to other NLDAS forcing data. Precipitation data were adjusted by first determining the ratio of total yearly winter precipitation (October–May) from SNOTEL to that of NLDAS. Then, NLDAS precipitation was scaled by the corresponding ratio. This simple bias correction shows that, in general, NLDAS precipitation is less than that recorded at the studied SNOTEL sites (Pan et al., 2003); thus, a substantial increase in SWE can be seen in years and stations where SWE was very poorly modeled (e.g., Station #463). There are a few years in which NLDAS precipitation data were more than the total precipitation recorded at the station and, therefore, precipitation bias correction resulted in reduced simulated SWE when compared to the control model (e.g., water year 2004 at Station #356, water year 2008 at Station #539). However, the number of snow-covered days has not been affected significantly (red line in Fig. 3 and termed as “control-bias-corr”) with the bias correction.

## Evaluating the UEB snow model in the Noah Land-Surface Model

R. Sultana et al.

[Title Page](#)

[Abstract](#)

[Introduction](#)

[Conclusions](#)

[References](#)

[Tables](#)

[Figures](#)

[⏪](#)

[⏩](#)

[◀](#)

[▶](#)

[Back](#)

[Close](#)

[Full Screen / Esc](#)

[Printer-friendly Version](#)

[Interactive Discussion](#)



## Evaluating the UEB snow model in the Noah Land-Surface Model

R. Sultana et al.

[Title Page](#)

[Abstract](#)

[Introduction](#)

[Conclusions](#)

[References](#)

[Tables](#)

[Figures](#)

[⏪](#)

[⏩](#)

[◀](#)

[▶](#)

[Back](#)

[Close](#)

[Full Screen / Esc](#)

[Printer-friendly Version](#)

[Interactive Discussion](#)

Model bias can also increase at sites where additional snowdrifts can result from wind or at sites with precipitation under-catch. The Noah land-surface model does not incorporate any physical processes for the effect of wind drifts; consequently, no additional processing is done for cases when accumulated SWE exceeded accumulated rainfall. From this point on, the simulated SWE after bias correction will be referred to as the “control” run of the Noah LSM and will be used for evaluation of the modified approach, which is termed as “Noah- $T_s$ ” run.

Simulation of the Noah LSM modified with the UEB snow model is compared at SNO-TEL stations and is shown in Fig. 4. The modified Noah shows substantially improved SWE estimation in terms of increasing the amount of maximum SWE as well as delaying snowmelt. However, water year 2007 (a moderate La Niño year) experiences the least amount of snow in all of the stations compared to the other six years of study, and the improvement from the modified model is not significant compared to the control run because the modified model uses available energy to melt shallow depths (less than 0.1 m) of snow.

While the modified model enhanced SWE simulation by using the Noah LSM, it also shows delayed SWE melting in few years, for example, in water year 2004 at Stations #463 and #508 and in water year 2008 at Station #508. This late melting can be partly explained by comparing the simulated SWE by the control-bias-corr model and the control model (Fig. 4) at Station #508. At this station, NDLAS precipitation was more than that observed in 2004 and 2008 and, therefore, after precipitation bias correction, the control-bias-corr model predicted less snow than the control model. In general, forcing data from NLDAS, other than precipitation, are well validated but, at this location and in these years, forcing uncertainty may still prevail. Figure 5 shows the maximum and minimum daily temperatures observed at Stations #508 and #463 from 1 April to 20 May 2004. During this period, NLDAS temperature data were comparatively cooler than observation, but the difference in maximum air temperature can affect the snow-melting process and time (Hamlet et al., 2005).

## Evaluating the UEB snow model in the Noah Land-Surface Model

R. Sultana et al.

Title Page

Abstract

Introduction

Conclusions

References

Tables

Figures

⏪

⏩

◀

▶

Back

Close

Full Screen / Esc

Printer-friendly Version

Interactive Discussion

Nonetheless, the modified approach has improved SWE estimation. Figure 6 shows the components of water balance-precipitation, sublimation, and snowmelt for the winter of 2001–2002 at California SNOTEL stations #356, #508, #463, and #539. During the accumulation period, snow is lost because of both sublimation and snow melting but the later is the primary reason for control model's low SWE bias relative to the observation. As discussed earlier, the control model simulates snow melt whenever the temperature of the snowpack reaches freezing point, and then melt water immediately becomes runoff. On the contrary, in the modified approach, snowmelt commences only when the net energy relative to the melting point is positive and snow melting do not start until later in the spring season (Fig. 6d, h, l, and p). Loss of snow due to sublimation from modified Noah-Ts is less compared to control model, particularly during the period control model has simulated snow on the ground (Fig. 6c, g, k, and o). This is because; control model applies penman equation (Wang et al., 2010) to compute snow sublimation while the modified model uses turbulent heat flux equation (Tarboton, 1994).

In the modified model, liquid water holding capacity of the snowpack was considered before the melt water becomes runoff and the effect of the liquid water content is shown in Fig. 7. The modified model was simulated with 0 and 5 % liquid water content, and the difference in response is seen only during the ablation period. There is no significant change in melt outflow rate until the beginning of the melt period. The simulation run with 5 % liquid water-holding capacity delays the onset of snowmelt, compared to that of 0 % liquid water-holding capacity for less than a day to approximately a few days.

The modified model was also used to simulate snow at a Utah SNOTEL site (Station #1098) near the TWDEF forest and simulation result is shown in Fig. 8. At this site, the SWE predicted by the control model does not show strong negative bias unlike simulation at all the California SNOTEL sites, and completion of the snowmelt by the control model is later than the observation time. The modified model rectifies these problems by improving the amount of SWE, as well as taking into account the earlier onset of snowmelt. Near this site, snow surface temperature is recorded and in Fig. 9 compares

## Evaluating the UEB snow model in the Noah Land-Surface Model

R. Sultana et al.

[Title Page](#)

[Abstract](#)

[Introduction](#)

[Conclusions](#)

[References](#)

[Tables](#)

[Figures](#)

[⏪](#)

[⏩](#)

[◀](#)

[▶](#)

[Back](#)

[Close](#)

[Full Screen / Esc](#)

[Printer-friendly Version](#)

[Interactive Discussion](#)

simulated snow-surface temperature and outgoing long-wave energy with that of observation for the first ten days of May 2009. Both the control and modified model have shown reasonable agreement with the observed surface temperature cycle although the control model simulates a colder snowpack. This is possibly because snow albedo at this site is relatively high (0.76) when compared to that of the California stations. As a result, snow-melt events are initiated later. In contrast, during the accumulation period, the modified model simulates SWE close to the observation, although melts the snowpack few days earlier than observation time.

At the California SNOTEL sites, neither the snow-surface temperature nor the energy flux measurement are available; hence, a comparison between the control model and the modified model simulated snow-surface temperature and turbulent fluxes at SNOTEL Station #356, as shown in Fig. 10. During the month of April 2002, there is no significant difference between the simulated surface temperature of the control model and that of the modified model, although the former is simulating a colder surface compared to the modified model (Fig. 10a). Therefore, latent heat flux computed by the modified model is larger compared to that of the control model (Fig. 10e). The differences in sensible heat flux (Fig. 10c) and outgoing long-wave radiation (Fig. 10d) between the control model and the modified model are found to be small. However, a significant difference between the models can be seen in the snow-melt outflow rate (Fig. 10b). During this time period, in the control model number of melt events reduced the snowpack while modified model did not simulate any snowmelt.

An additional review of the effectiveness of the modified model in predicting maximum SWE is presented in Fig. 11, where maximum-modeled SWE as a percentage of ground-observed maximum SWE is shown at the four California SNOTEL stations for seven years of the study period. Although precipitation bias correction improved model SWE estimation, the overall enhancement in maximum SWE prediction by the modified model is evident (Fig. 11). A similar comparison is shown in Fig. 11, which includes the 21 California SNOTEL stations over the Sierra Nevada Mountains. The control model can reasonably predict SWE at locations where maximum SWE is rel-

atively less ( $SWE_{max} < 500$  mm). However, bias is more pronounced at locations with higher snowfall. The modified model has enhanced SWE estimation at all locations, but improvement is more prominent for observation stations where the maximum snowfall is between 500–1000 mm.

5 Additionally, the modified model's overall predictive power to simulate SWE is described by the Nash–Sutcliffe coefficient, shown in Table 2. For all stations, the value of the coefficient is almost always positive, which again supports the accuracy of the modified model in SWE estimation.

10 Snow-covered ground can affect soil temperature, as well as moisture content of the underlying soil. Although the scope of the paper is only limited to evaluating alternative processes for snow temperature and snowmelt, soil temperature and moisture from the control and modified models are compared with respective observations at the SNOTEL stations. Figure 13 shows the comparison of model output with observed soil temperature and soil moisture 5 mm below the ground at Stations #508 and #463. The control model predicts less snow and, therefore, the ground is more exposed to the cooler atmosphere (during the month of January in Fig. 12c and d). But, the ground is warmer and soil temperature is above the freezing point during most of the snow season. The observation sites initialize the measuring instrument at every water year and so for the first few months, the soil moisture is recorded as zero. Control model, with frequent snow melt event, control model simulates a higher soil moisture fraction while soil moisture content is reduced significantly (Fig. 12e and f) in the modified Noah model because of less snow melt event during the snow season. Additional analysis of improving the soil temperature and moisture content is suggested but is beyond the scope of this study.

## HESSD

10, 13363–13406, 2013

### Evaluating the UEB snow model in the Noah Land-Surface Model

R. Sultana et al.

Title Page

Abstract

Introduction

Conclusions

References

Tables

Figures

⏪

⏩

◀

▶

Back

Close

Full Screen / Esc

Printer-friendly Version

Interactive Discussion

## 5 Conclusions

The Noah LSM has been identified to under predict snow-water equivalent throughout the snow season and melt away all the snow early in spring. The control model simulates snowpack as a single layer and estimates the snow-surface temperature based on the energy flux on the snow surface and the air temperature above the snow surface. When the snowpack is at freezing temperature ( $0^{\circ}\text{C}$ ), snow starts to melt. In reality, snow temperature is not the only determining factor for snow melt. To begin snow melting, the entire snowpack is required to be isothermal and the modified Noah model, like UEB model, determines this by accounting for internal energy of the snowpack. This melt water does not instantly become runoff but remains within the warm snowpack up to the liquid water-holding capacity. Once this water-holding capacity is exceeded, snowmelt becomes runoff.

In addition to considering internal energy of the snowpack, force-restore method was applied in modified Noah model to compute snow-surface temperature. The results show that snow surface temperature is similar and sometimes warmer than the temperature computed by the control model and thus did not add any benefits to the model. The primary factor for improvement in modified model's SWE estimation is the regulating melt events.

The new scheme adds only two prognostic variables and is compatible with other physical processes within the model. One effort of this study was to preserve the simplicity of the Noah model but remove model deficiencies. In general, the modified Noah LSM outperformed the control model.

# HESSD

10, 13363–13406, 2013

## Evaluating the UEB snow model in the Noah Land-Surface Model

R. Sultana et al.

[Title Page](#)

[Abstract](#)

[Introduction](#)

[Conclusions](#)

[References](#)

[Tables](#)

[Figures](#)

[⏪](#)

[⏩](#)

[◀](#)

[▶](#)

[Back](#)

[Close](#)

[Full Screen / Esc](#)

[Printer-friendly Version](#)

[Interactive Discussion](#)

Surface-energy balance at the snow surface:

$$R_{\text{dn}} - \varepsilon\sigma T_s^4 = G + H + \beta L_v E_p - L_f P_r + P_r c_p (T_s - T_o)$$

$$R_{\text{dn}} - \varepsilon\sigma T_s^4 = k \frac{T_s - T_{\text{soil}}}{\Delta z} + \rho c_p C_H (T_s - \theta_o) + \beta L_v E_p - L_f P_r + P_r c_p (T_s - T_o)$$

where  $T_s$  is the surface temperature (K),  $T_o$  is the air temperature (K),  $k$  is the thermal conductivity of soil,  $\rho$  is the density of the air,  $C_H$  is the turbulent-exchange coefficient,  $\Delta z$  is the depth of the snowpack plus half of the top soil layer,  $T_{\text{soil}}$  is the soil temperature at half of the top soil layer,  $R_{\text{dn}}$  is the net short-wave radiation,  $\varepsilon$  is the emissivity of the surface,  $\sigma$  is the Stephen Boltzman's constant,  $L_f$  is the latent heat of fusion,  $c_p$  is the specific heat of air,  $P_r$  is the precipitation,  $\theta_o$  is the potential air temperature above the ground (usually at 2 m),  $L_v$  is the latent heat of condensation, and  $E_p$  is the potential evaporation rate.

Applying Taylor's expansion on  $\varepsilon\sigma T_s^4$ :

$$R_{\text{dn}} - \varepsilon\sigma T_o^4 - 4\varepsilon\sigma T_o^4 \frac{T_s - T_o}{T_o} = k \frac{T_s - T_{\text{soil}}}{\Delta z} + \rho c_p C_H [(T_s - T_o) - (\theta_o - T_o)] + \beta L_v E_p - L_f P_r + P_r c_p (T_s - T_o).$$

**Evaluating the UEB snow model in the Noah Land-Surface Model**

R. Sultana et al.

[Title Page](#)

[Abstract](#)   [Introduction](#)

[Conclusions](#)   [References](#)

[Tables](#)   [Figures](#)

[⏪](#)   [⏩](#)

[◀](#)   [▶](#)

[Back](#)   [Close](#)

[Full Screen / Esc](#)

[Printer-friendly Version](#)

[Interactive Discussion](#)



Dividing both sides by  $\rho c_p C_H$ :

$$\frac{R_{dn} - \varepsilon \sigma T_o^4}{\rho c_p C_H} - \frac{4\varepsilon \sigma T_o^4}{\rho c_p C_H} \frac{T_s - T_o}{T_o} = \frac{k}{\rho c_p C_H} \frac{T_s - T_{soil}}{\Delta z} + (T_s - T_o) - (\theta_o - T_o) + \frac{\beta L_V E_p}{\rho c_p C_H} + \frac{-L_f P_r + P_r c_p (T_s - T_o)}{\rho c_p C_H}$$

$$\frac{R_{dn} - \varepsilon \sigma T_o^4}{\rho c_p C_H} + (\theta_o - T_o) - \frac{\beta L_V E_p}{\rho c_p C_H} - \frac{-L_f P_r}{\rho c_p C_H} = \left[ \frac{4\varepsilon \sigma T_o^4}{\rho c_p C_H T_o} + 1 + \frac{P_r c_p}{\rho c_p C_H} \right] (T_s - T_o) + \frac{k}{\rho c_p C_H} \frac{T_s - T_{soil}}{\Delta z}$$

setting,  $r = \frac{4\varepsilon \sigma T_o^4}{\rho c_p C_H T_o} + \frac{P_r c_p}{\rho c_p C_H}$

$$\frac{\frac{R_{dn} - \varepsilon \sigma T_o^4}{\rho c_p C_H} + (\theta_o - T_o) - \frac{\beta L_V E_p}{\rho c_p C_H} - \frac{-L_f P_r}{\rho c_p C_H}}{r + 1} = (T_s - T_o) + \frac{k}{\rho c_p C_H (r + 1)} \frac{T_s - T_{soil}}{\Delta z}$$

$$= \left( 1 + \frac{k}{\rho c_p C_H (r + 1) \Delta z} \right) T_s - T_o - \frac{k}{\rho c_p C_H (r + 1) \Delta z} T_{soil}$$

$$T_s = \frac{T_o + \frac{K}{\rho c_p C_H (r + 1) \Delta z} T_{soil} + \frac{R_{dn} - \varepsilon \sigma T_o^4 + L_f P_r c_p + \theta_o - T_o - \frac{\beta L_V E_p}{\rho c_p C_H}}{r + 1}}{1 + \frac{K}{\rho c_p C_H (r + 1) \Delta z}}$$

where:

$$r = \frac{4\varepsilon \sigma T_o^4}{\rho c_p C_H T_o} + \frac{P_r c_p}{\rho c_p C_H}$$

## Evaluating the UEB snow model in the Noah Land-Surface Model

R. Sultana et al.

Title Page

Abstract

Introduction

Conclusions

References

Tables

Figures

◀

▶

◀

▶

Back

Close

Full Screen / Esc

Printer-friendly Version

Interactive Discussion



## Evaluating the UEB snow model in the Noah Land-Surface Model

R. Sultana et al.

Title Page

Abstract

Introduction

Conclusions

References

Tables

Figures

⏪

⏩

◀

▶

Back

Close

Full Screen / Esc

Printer-friendly Version

Interactive Discussion

where  $T_s$  is the snow temperature (K),  $T_o$  is the air temperature (K),  $K$  is the thermal conductivity of soil,  $\rho$  is the density of the air,  $C_H$  is the turbulent-exchange coefficient,  $\Delta z$  is the depth of the snowpack plus half of the top soil layer,  $T_{soil}$  is the soil temperature at half-depth of the top soil layer,  $R_{dn}$  is the net short-wave radiation,  $\varepsilon$  is the emissivity of the surface,  $\sigma$  is the Stephen Boltzman's constant,  $L_f$  is the latent heat of fusion,  $c_p$  is the specific heat of air,  $P_r$  is the precipitation,  $\theta_o$  is the potential air temperature above the ground (usually at 2 m),  $L_v$  is the latent heat of condensation, and  $E_p$  is the potential evaporation rate.

*Acknowledgements.* Primary support for this study was provided by NOAA CPPA program, grant NA08OAR4310876. Partial support was provided by the NASA JPL, grant NMR711086 with JPL sub-Contract 1401333. The authors would like to thank Vinod Mahat for his assistance with UEB model code, and David Tarboton, along with two anonymous reviewers, for their thorough review and comments.

## References

- Albert, M. R. and Krajleski, G. N.: A fast, physically-based point snow melt model for distributed applications, *Hydrol. Process.*, 12, 1809–1824, 1998.
- Anderson, E. A.: A Point Energy and Mass Balance Model of a Snow Cover, NOAA Technical Report NWS 19, US Department of Commerce, Silver Springs, Maryland, 150 pp., 1976.
- Arons, E. M. and Colbeck, S. C.: Geometry of heat and mass transfer in dry snow: a review of theory and experiment, *Rev. Geophys.*, 33, 463–493, 1995.
- Bengtsson, L.: Percolation of meltwater through a snowpack, *Cold Reg. Sci. Technol.*, 6, 73–81, 1982.
- Bhumralkar, C. M.: Numerical experiments on the computation of ground surface temperature in an atmospheric circulation model, *J. Appl. Meteorol.*, 14, 1246–1258, 1975.
- Barlage, M., Chen, F., Tewari, M., Ikeda, K., Gochis, D., Dudhia, J., Rasmussen, R., Livneh, B., Ek, M., and Mitchell, K.: Noah land surface model modifications to improve snowpack prediction in the Colorado Rocky Mountains, *J. Geophys. Res.*, 115, D22101, doi:10.1029/2009JD013470, 2010.

## Evaluating the UEB snow model in the Noah Land-Surface Model

R. Sultana et al.

Title Page

Abstract

Introduction

Conclusions

References

Tables

Figures

⏪

⏩

◀

▶

Back

Close

Full Screen / Esc

Printer-friendly Version

Interactive Discussion

- Chen, F. and Dudhia, J.: Coupling an advanced land surface hydrology model with the Penn State-NCAR MM5 modeling system, Part 1: Model implementation and sensitivity, *Mon. Weather Rev.*, 129, 569–585, doi:10.1175/1520-0493(2001)129<0587:CAALSH>2.0.CO;2, 2001.
- 5 Chen, F., Mitchell, K., Schaake, J., Xue, Y., Pan, H., Koren, V., Duan, Y., Ek, M., and Betts, A.: Modeling of land surface evaporation by four schemes and comparison with FIFE observations, *J. Geophys. Res.*, 101, 7251–7268, doi:10.1029/95JD02165, 1996.
- Chen, F., Manning, K. W., LeMone, M. A., Trier, S. B., Alfieri, J. G., Roberts, R., Tewari, M., Niyogi, M., D., Horst, T. W., Oncley, S. P., Basara, J. B., and Blanken, P. D.: Description  
10 and evaluation of the characteristics of the NCAR High-resolution land data assimilation system, *J. Appl. Meteorol. Clim.*, 46, 694–713, 2007.
- Colbeck, S. C.: A theory of water percolation in snow, *J. Glaciol.*, 11, 369–385, 1972.
- Colbeck, S. C. and Anderson, E. A.: The permeability of a melting snow cover, *Water Resour. Res.*, 18, 904–908, 1982.
- 15 Cosgrove, B. A., Lohmann, D., Mitchell, K. E., Houser, P. R., Wood, E. F., Schaake, J. S., Robock, A., Marshall, C., Sheffield, J., Duan, Q. Y., Luo, L. F., Higgins, R. W., Pinker, R. T., Tarpley, J. D., and Meng, J.: Real-time and retrospective forcing in the North American Land Data Assimilation System (NLDAS) project, *J. Geophys. Res.*, 108, 8842, doi:10.1029/2002JD003118, 2003.
- 20 Dai, Y., Zeng, X., Dickinson, R. E., Baker, I., Bonan, G. B., Bosilovich, M. G., Denning, A. S., Dirmeyer, P. A., Houser, P. R., Niu, G., Oleson, K. W., Schlosser, C. A., and Yang, Z.-L.: The common land model (CLM), *B. Am. Meteorol. Soc.*, 84, 1013–1023, 2003.
- Deardorff, J. W.: Efficient prediction of ground surface temperature and moisture with inclusion of a layer of vegetation, *J. Geophys. Res.*, 83, 1889–1903, 1978.
- 25 Denoth, A., Foglar, A., Weiland, P., Matzler, C., Aebischer, H., Tiuri, M., and Sihvola, A.: A comparative study of instruments for measuring the liquid water content of snow, *J. Appl. Phys.*, 56, 2154–2160, 1984.
- Dickinson, R. E.: The force-restore method for surface temperature and its generalization, *J. Climate*, 1, 1086–1097, 1988.
- 30 Dickinson, R. E., Henderson-Sellers, A., Kennedy, P. J., and Giogi, F.: Biosphere–Atmosphere Transfer Scheme (BATS) Version 1e Coupled to the NCAR Community Climate Model, NCAR Technical Note TN-387STR, National Center for Atmospheric Research, Boulder, Colorado, 1993.

## Evaluating the UEB snow model in the Noah Land-Surface Model

R. Sultana et al.

[Title Page](#)

[Abstract](#)

[Introduction](#)

[Conclusions](#)

[References](#)

[Tables](#)

[Figures](#)

[⏪](#)

[⏩](#)

[◀](#)

[▶](#)

[Back](#)

[Close](#)

[Full Screen / Esc](#)

[Printer-friendly Version](#)

[Interactive Discussion](#)

- Dingman, S. L.: Physical Hydrology, Waveland Press Inc., Illinois, 645 pp., 2009.
- Dunne, T., Price, A. G., and Colbeck, S. C.: The generation of runoff from subarctic snowpacks, *Water Resour. Res.*, 12, 677–685, 1976.
- Eagleson, P. S.: Dynamic Hydrology, McGraw-Hill, New York, 462 pp., 1970.
- 5 Ek, M. B., Mitchell, K., Lin, E. Y., Rogers, E., Grunmann, P., Koren, V., Gayno, G., and Tarp-  
ley, J. D.: Implementation of Noah land surface model advances in the National Centers for  
Environmental Prediction operational mesoscale Eta model, *J. Geophys. Res.*, 108, 8851,  
doi:10.1029/2002JD003296, 2003.
- 10 Gao, Z., Horton, R., Wang, L., Liu, H., and Wen, J.: An improved force-restore method  
for soil temperature prediction, *Eur. J. Soil Sci.*, 59, 972–981, doi:10.1111/j.1365-  
2389.2008.01060.x, 2008.
- Gray, D. M. and Male, D. H.: *Handbook of Snow, Principles, Processes, Management & Use*,  
Pergamon Press, New York, 1981.
- 15 Hamlet, A. F., Mote, P. W., Clark, M. P., and Lettenmaier, D. P.: Effects of temperature and  
precipitation variability on snowpack trends in the western United States, *J. Climate*, 18,  
4545–4561, 2005.
- Hu, Z. and Islam, S.: Prediction of ground surface temperature and soil moisture content by the  
force-restore method, *Water Resour. Res.*, 31, 2531–2539, 1995.
- 20 Iida, T., Ukei, K., Tsukahara, H., and Kajihara, A.: Point physical model of movement of ions  
through natural snow cover, *J. Hydrol.*, 235, 170–182, 2000.
- Jiang, X., Wiedinmyer, C., Chen, F., Yang, Z. L., and Lo, J. C. F.: Predicted impacts of climate  
and land use change on surface ozone in the Houston, Texas, area, *J. Geophys. Res.*, 113,  
D20312, doi:10.1029/2008JD009820, 2008.
- Jin, J. and Miller, N. L.: Analysis of the impact of snow on daily weather variability in mountain-  
ous regions using MM5, *J. Hydrometeorol.*, 8, 245–258, 2007.
- 25 Jin, J., Gao, X., Yang, Z. L., Bales, R. C., Sorooshian, S., Dickinson, R. E., Sun, S. F., and  
Wu, G. X.: Comparative analyses of physically based snowmelt models for climate simula-  
tions, *J. Climate*, 12, 2643–2657, 1999.
- 30 Jordan, R.: A one-dimensional temperature model for a snow cover: technical documentation  
for SNThER M.89, Special Report 91–16, US Army Corps of Engineers Cold Regions Re-  
search and Engineering Laboratory, Hanover, New Hampshire, 49 pp., 1991.

**Evaluating the UEB  
snow model in the  
Noah Land-Surface  
Model**

R. Sultana et al.

[Title Page](#)[Abstract](#)[Introduction](#)[Conclusions](#)[References](#)[Tables](#)[Figures](#)[⏪](#)[⏩](#)[◀](#)[▶](#)[Back](#)[Close](#)[Full Screen / Esc](#)[Printer-friendly Version](#)[Interactive Discussion](#)

- Kahan, D. S., Xue, Y., and Allen, S. J.: The impact of vegetation and soil parameters in simulations of surface energy and water balance in the semi-arid Sahel: a case study using SEBEX and HAPEX-Sahel data, *J. Hydrol.*, 320, 238–259, 2006.
- Kattlemann, R.: Methods of estimating liquid water storage in snow, *West. Snow Conf.*, 14–16 April, Vancouver, British Columbia, Canada, 158–161, 1987.
- Kendra, J. R., Ulaby, F. T., and Sarabandi, K.: Snow probe for in situ determination of wetness and density, *IEEE T. Geosci. Remote*, 32, 1152–1159, 1994.
- Koren, V., Schaake, J. C., Mitchell, K. E., Duan, Q. Y., Chen, F., and Baker, J.: A parameterization of snowpack and frozen ground intended for NCEP weather and climate models, *J. Geophys. Res.*, 104, 19569–19585, doi:10.1029/1999JD900232, 1999.
- Leung, L. R., Done, J., Dudhia, J., Henderson, T., Vertenstein, M., and Kuo, B.: Preliminary results of WRF for regional climate simulations, Paper presented at the Workshop on Research Needs and Directions of Regional Climate Modeling Using WRF and CCSM, National Center for Atmospheric Research, Boulder, Colorado, available at: <http://nldr.library.ucar.edu/repository/assets/osgc/OSGC-000-000-011-917.pdf> (last access: 24 February 2013), 2005.
- Leung, L. R., Kuo, Y. H., and Tribbia, J.: Research needs and directions of regional climate modeling using WRF and CCSM, *B. Am. Meteorol. Soc.*, 87, 1747–1751, doi:10.1175/BAMS-87-12-1747, 2006.
- Lin, J. D.: On the force-restore method for prediction of ground surface temperature, *J. Geophys. Res.*, 85, 3251–3254, 1980.
- Livneh, B., Xia, Y., Mitchell, K. E., Ek, M. B., and Lettenmaier, D. P.: Noah LSM snow model diagnostics and enhancements, *J. Hydrometeorol.*, 11, 721–738, 2009.
- Luce, C. H. and Tarboton, D. G.: A modified force-restore approach to modeling snow surface heat fluxes, the 69th Ann. Meeting of the West. Snow Conf., 16–19 April, Sun Valley, Idaho, 2001.
- Luce, C. H. and Tarboton, D. G.: Evaluation of alternative formulae for calculation of surface temperature in snowmelt models using frequency analysis of temperature observations, *Hydrol. Earth Syst. Sci.*, 14, 535–543, doi:10.5194/hess-14-535-2010, 2010.
- Lundquist, J. D. and Flint, A. L.: Onset of snowmelt and streamflow in 2004 in the Western United States: how shading may affect spring streamflow timing in a warmer world, *J. Hydrometeorol.*, 7, 1199–1217, 2006.
- Luo, L., Robock, A., Mitchell, K. E., Houser, P. R., Wood, E. F., Schaake, J. C., Lohmann, D., Cosgrove, B., Wen, F., Sheffield, J., Duan, Q., Higgins, R. W., Pinker, R. T., and Tarp-

## Evaluating the UEB snow model in the Noah Land-Surface Model

R. Sultana et al.

[Title Page](#)

[Abstract](#)

[Introduction](#)

[Conclusions](#)

[References](#)

[Tables](#)

[Figures](#)

[⏪](#)

[⏩](#)

[◀](#)

[▶](#)

[Back](#)

[Close](#)

[Full Screen / Esc](#)

[Printer-friendly Version](#)

[Interactive Discussion](#)

ley, J. D.: Validation of the North American Land Data Assimilation System (NLDAS) retrospective forcing over the southern Great Plains, *J. Geophys. Res.*, 108, 8843, doi:10.1029/2002JD003246, 2003.

5 Mahfouf, J.-F., Manzi, A. O., Noilhan, J., Giordani, H., and Déqué, M.: The land surface scheme ISBA within the Météo-France climate model ARPEGE, Part 1: Implementation and preliminary results, *J. Climate*, 8, 2039–2057, 1995.

Male, D. H. and Gray, D. M.: Snowcover ablation and runoff, in: *Handbook of Snow, Principles, Processes, Management and Use*, edited by: Gray, D. M. and Male, D. H., Pergamon Press, Toronto, New York, 360–436, 1981.

10 Mitchell, K. E., Lohmann, D., Houser, P. R., Wood, E. F., Schaake, J. C., Robock, A., Cosgrove, B. A., Sheffield, J., Duan, Q., Luo, L., Higgins, R. W., Pinker, R. T., Tarpley, J. D., Lettenmaier, D. P., Marshall, C. H., Entin, J. K., Pan, M., Shi, W., Koren, V., Meng, J., Ramsay, B. H., and Bailey, A. A.: The multi-institutional North American Land Data Assimilation System (NLDAS): utilizing multiple GCIP products and partners in a continental distributed hydrological modeling system, *J. Geophys. Res.*, 109, D07S90, doi:10.1029/2003JD003823, 2004.

Niu, G.-Y., Yang, Z. L., Mitchell, K. E., Chen, F., Ek, M. B., Barlage, M., Kumar, A., Manning, K., Niyogi, D., Rosero, E., Tewarr, M., and Xia, Y.: The community Noah land surface model with multiparameterization options (Noah-MP): 1. Model description and evaluation with local-scale measurements, *J. Geophys. Res.*, 116, D12109, doi:10.1029/2010JD015139, 2011.

20 Noilhan, J. and Planton, S.: A simple parameterization of land surface processes for meteorological models, *Mon. Weather Rev.*, 117, 536–549, 1989.

Pan, M., Sheffield, J., Wood, E. F., Mitchell, K. E., Houser, P. R., Schaake, J. C., Robock, A., Lohmann, D., Cosgrove, B., Duan, Q., Luo, L., Higgins, R. W., Pinker, R. T., and Tarpley, J. D.: Snow process modeling in the North American Land Data Assimilation System (NLDAS): 2. Evaluation of model simulated snow water equivalent, *J. Geophys. Res.*, 108, 8850, doi:10.1029/2003JD003994, 2003.

25 Pederson, G. T., Gray, S. T., Ault, T., Marsh, W., Farge, D. B., Bunn, A. G., Woodhouse, C. A., and Graumlich, L. J.: Climatic controls on the snowmelt hydrology of the northern Rocky Mountains, *J. Climate*, 24, 1666–1687, 2010.

Peters-Lidard, C. D., Houser, P. R., Tian, Y., Kumar, S. V., Geiger, J., Olden, S., Lighty, L., Doty, B., Dirmeyer, P., Adams, J., Mitchell, K., Wood, E. F., and Sheffield, J.: High performance

## Evaluating the UEB snow model in the Noah Land-Surface Model

R. Sultana et al.

[Title Page](#)

[Abstract](#)

[Introduction](#)

[Conclusions](#)

[References](#)

[Tables](#)

[Figures](#)

[⏪](#)

[⏩](#)

[◀](#)

[▶](#)

[Back](#)

[Close](#)

[Full Screen / Esc](#)

[Printer-friendly Version](#)

[Interactive Discussion](#)

Earth system modeling with NASA/GSFC's Land Information System, *Innov. Syst. Softw. Eng.*, 3, 157–165, doi:10.1007/s11334-007-0028-x, 2007.

Peterson, D., Smith, R., Hager, S., Cayan, D., and Dettinger, M.: Air Temperature and Snowmelt Discharge Characteristics, Merced River at Happy Isles, Yosemite National Park, Central Sierra Nevada, PACLIM Conference Proceedings, 6–9 April 2003, Pacific Grove, California, 53–64, 2003.

Pinker, R. T., Tarpley, J. D., Laszlo, I., Mitchell, K. E., Houser, P. R., Wood, E. F., Schaake, J. C., Robock, A., Lohmann, D., Cosgrove, B. A., Sheffield, J., Duan, Q., Luo, L., and Higgins, R. W.: Surface radiation budgets in support of the GEWEX Continental Scale International Project (GCIP) and the GEWEX Americas Prediction Project (GAPP), including the North American Land Data Assimilation System (NLDAS) project, *J. Geophys. Res.*, 108, 8844, doi:10.1029/2002JD003301, 2003.

Ren, D. and Xue, M.: A revised force-restore model for land surface modeling, *J. Appl. Meteorol.*, 43, 1768–1782, 2004.

Schlosser, C. A., Slater, A. G., Robock, A., Pitman, A. J., Vinnikov, K. Y., Henderson-Sellers, A., Speranskaya, N. A., Mitchell, K., and the PILPS 2(D) contributors: Simulations of a boreal grassland hydrology at Valdai, Russia: PILPS Phase 2(D), *Mon. Weather Rev.*, 128, 301–321, 2000.

Sellers, P. J., Randall, D. A., Collatz, G. J., Berry, J. A., Field, C. B., Dazlich, D. A., Zhang, C., Collelo, G. D., and Bounoua, L.: A revised land surface parameterization (SiB2) for atmospheric GCMs, Part 1: Model formulation, *J. Climate*, 9, 676–705, 1996.

Serreze, M. C., Clark, M. P., Armstrong, R. L., McGinnis, D. A., and Pulwarty, R. S.: Characteristics of the western United States snowpack from snowpack telemetry (SNOTEL) data, *Water Resour. Res.*, 35, 2145–2160, 1999.

Sheffield, J., Pan, M., Wood, E. F., Mitchell, K. E., Houser, P. R., Schaake, J. C., Robock, A., Lohmann, D., Cosgrove, B., Duan, Q., Luo, L., Higgins, R. W., Pinker, R. T., Tarpley, R. T., Tarpley, D., and Ramsay, B. H.: Snow process modeling in the North American Land Data Assimilation System (NLDAS): 1. Evaluation of model-simulated snow cover extent, *J. Geophys. Res.*, 108, 8849, doi:10.1029/2002JD003274, 2003.

Slater, A. G., Schlosser, C. A., Desborough, C. E., Pitman, A. J., Henderson-Sellers, A., Robock, A., Vinnikov, K. Y., Mitchell, K., Boone, A., Braden, H., Chen, F., Cox, P. M., De Rosnay, P., Dickinson, R. E., Dai, Y.-J., Duan, Q., Entin, J., Etchevers, P., Gedney, N., Gusev, Ye. M., Habets, F., Kim, J., Koren, V., Kowalczyk, E. A., Nasonova, O. N., Noilhan, J.,

## Evaluating the UEB snow model in the Noah Land-Surface Model

R. Sultana et al.

Title Page

Abstract

Introduction

Conclusions

References

Tables

Figures

⏪

⏩

◀

▶

Back

Close

Full Screen / Esc

Printer-friendly Version

Interactive Discussion

Schaake, S., Shmakin, A. B., Smirnova, T. G., Versegny, D., Wetzel, P., Xue, Y., Lang, Z.-L., and Zeng, Q.: The representation of snow in land surface schemes: results from PILPS 2(d), *J. Hydrometeorol.*, 2, 7–25, 2001.

Tarboton, D. G.: Measurements and Modeling of Snow Energy Balance and Sublimation from Snow, Reports, Paper 61, available at: [http://digitalcommons.usu.edu/water\\_rep/61](http://digitalcommons.usu.edu/water_rep/61) (last access: 9 December 2012), 1994.

Tarboton, D. G. and Luce, C. H.: Utah Energy Balance Snow Accumulation and Melt Model (UEB), Computer model technical description and users guide, Utah Water Research Laboratory and USDA Forest Service Intermountain Research Station, available at: <http://www.engineering.usu.edu/dtarb/> (last access: 2 February 2010), 1996.

Tarboton, D. G., Chowdhury, T. G., and Jackson, T. H.: A Spatially Distributed Energy Balance Snowmelt Model, Reports, Paper 60, available at: [http://digitalcommons.usu.edu/water\\_rep/60](http://digitalcommons.usu.edu/water_rep/60) (last access: 9 December 2012), 1994.

Tarboton, D. G., Chowdhury, T. G., and Jackson, T. H.: A Spatially Distributed Energy Balance Snowmelt Model, in *Biogeochemistry of Seasonally Snow-Covered Catchments*, Proceedings of a Boulder Symposium, 3–14 July, IAHS Publ., 228, 141–155, 1995.

US Army Corps of Engineers: Summary report of the snow investigations: snow hydrology, North Pac. Div., Portland, OR, 1956.

Yang, Z. L., Niu, G. Y., Mitchell, K. E., Chen, F., Ek, M. B., Barlage, M., Longuevergne, L., Manning, K., Niyogi, D., Tewari, M., and Xia, Y.: The community Noah land surface model with multiparameterization options (Noah-MP): 2. Evaluation over global river basins, *J. Geophys. Res.*, 116, D12110, doi:10.1029/2010JD015140, 2011.

Yerdelen, C. and Acar, R.: Study on prediction of snowmelt using energy balance equations and comparing with regression method in the Eastern part of Turkey, *J. Sci. Ind.*, 64, 520–528, 2005.

You, J.: Snow hydrology: the parameterization of subgrid processes within a physically based snow energy and mass balance model, Ph. D. Dissertation, Civil and Environmental Engineering, Utah State University, Logan, UT, 2004.

Wang, Z., Zeng, X., and Decker, M.: Improving snow processes in the Noah land model, *J. Geophys. Res.*, 115, D20108, doi:10.1029/2009JD013761, 2010.

Zanotti, F., Endrizzi, S., Bertoldi, G., and Rigon, R.: The GEOTOP snow model, 61st Eastern Snow Conference, Portland, ME, 2004.

**HESSD**

10, 13363–13406, 2013

**Evaluating the UEB  
snow model in the  
Noah Land-Surface  
Model**

R. Sultana et al.

[Title Page](#)[Abstract](#)[Introduction](#)[Conclusions](#)[References](#)[Tables](#)[Figures](#)[I◀](#)[▶I](#)[◀](#)[▶](#)[Back](#)[Close](#)[Full Screen / Esc](#)[Printer-friendly Version](#)[Interactive Discussion](#)**Table 1.** Elevation and annual rainfall at four SNOTEL sites for June 2001–June 2008.

SNOTEL stations	Elevation (m)	Average annual rainfall (mm)
#356	2456	1003
#508	2370	751
#463	2338	1446
#539	2135	729

## Evaluating the UEB snow model in the Noah Land-Surface Model

R. Sultana et al.

**Table 2.** Nash–Sutcliffe efficiency coefficients for the modified model (the efficiency coefficients for the control model are shown in parentheses) at four SNOTEL stations.

Station	2001–2002	2002–2003	2003–2004	2004–2005	2005–2006	2006–2007	2007–2008
#356	0.5865 (−1.0433)	0.8655 (−0.4183)	0.6464 (−0.1951)	0.6489 (0.0574)	0.446 (0.0174)	0.6278 (0.5267)	0.6955 (0.068)
#508	0.81 (−0.1853)	0.107 (−1.09)	0.6625 (0.1878)	0.8599 (−0.1515)	0.9604 (0.6565)	0.6684 (0.6155)	0.8499 (0.7154)
#463	0.2375 (−1.34)	0.7586 (−1.6837)	0.4447 (−0.4926)	0.5949 (−0.8203)	0.1315 (−0.2948)	0.5727 (0.5431)	0.6461 (−0.1503)
#539	0.0620 (−1.0426)	−0.1145 (−0.9057)	0.4312 (−0.6300)	0.1109 (−0.8621)	0.4861 (−0.3793)	0.4186 (0.4049)	0.2296 (−0.6509)

Title Page

Abstract

Introduction

Conclusions

References

Tables

Figures

⏪

⏩

◀

▶

Back

Close

Full Screen / Esc

Printer-friendly Version

Interactive Discussion

## Evaluating the UEB snow model in the Noah Land-Surface Model

R. Sultana et al.

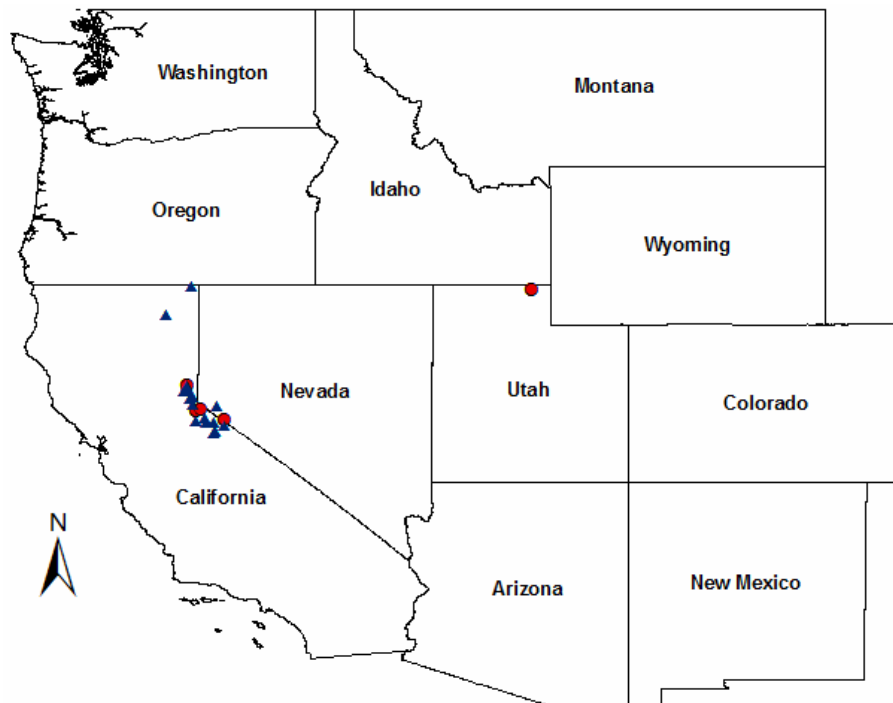


**Fig. 1.** Location of 23 SNOTEL stations (shown in circle and triangle) used for this study. The model results are shown in detail at locations marked by circles.

[Title Page](#)[Abstract](#)[Introduction](#)[Conclusions](#)[References](#)[Tables](#)[Figures](#)[⏪](#)[⏩](#)[◀](#)[▶](#)[Back](#)[Close](#)[Full Screen / Esc](#)[Printer-friendly Version](#)[Interactive Discussion](#)

## Evaluating the UEB snow model in the Noah Land-Surface Model

R. Sultana et al.

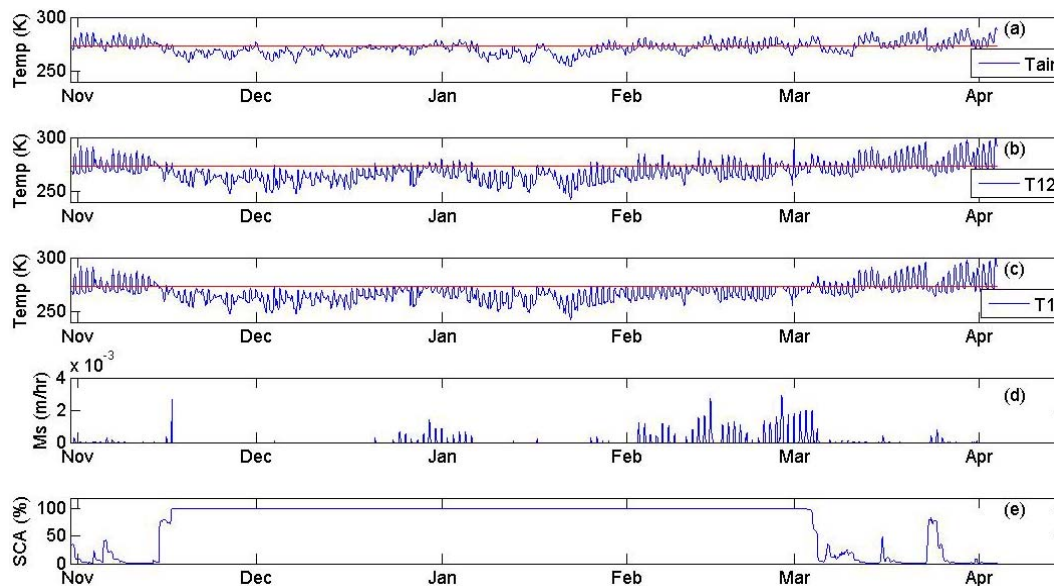


**Fig. 2.** Graphical example describing the Noah LSM's snow-temperature estimation process and how the snow-melt events are initiated: **(a)** air temperature  $T_{\text{air}}$ , **(b)** temperature  $T_{12}$  estimated from the surface-energy balance, **(c)** resultant snow-skin temperature,  $T_1$ , **(d)** rate of snowmelt  $M_s$ , and **(e)** percentage of snow-cover area (SCA). The red lines in **(a)**, **(b)**, and **(c)** indicate 273.15 K.

[Title Page](#)
[Abstract](#)
[Introduction](#)
[Conclusions](#)
[References](#)
[Tables](#)
[Figures](#)
[◀](#)
[▶](#)
[◀](#)
[▶](#)
[Back](#)
[Close](#)
[Full Screen / Esc](#)
[Printer-friendly Version](#)
[Interactive Discussion](#)

## Evaluating the UEB snow model in the Noah Land-Surface Model

R. Sultana et al.

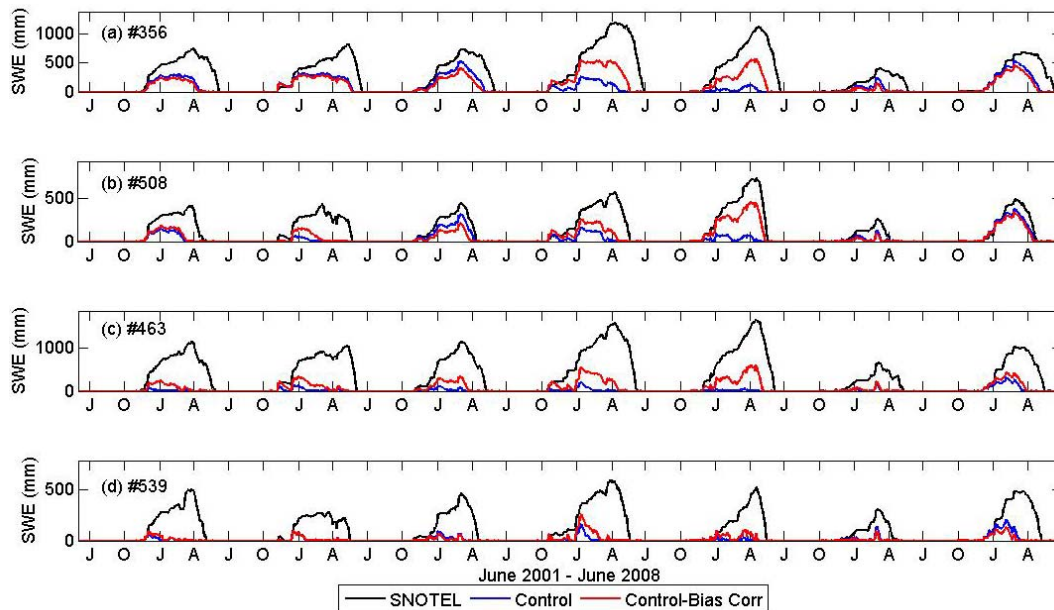


**Fig. 3.** Simulated SWE with NLDAS precipitation (blue line) and after precipitation bias correction (red line) are compared with observation (black line) sites: **(a)** #356, **(b)** #508, **(c)** #463, and **(d)** #539. Model run before precipitation bias correction is called “control”, and the model run after precipitation bias correction is called “control-bias corr”.

[Title Page](#)
[Abstract](#)
[Introduction](#)
[Conclusions](#)
[References](#)
[Tables](#)
[Figures](#)
[⏪](#)
[⏩](#)
[◀](#)
[▶](#)
[Back](#)
[Close](#)
[Full Screen / Esc](#)
[Printer-friendly Version](#)
[Interactive Discussion](#)

## Evaluating the UEB snow model in the Noah Land-Surface Model

R. Sultana et al.

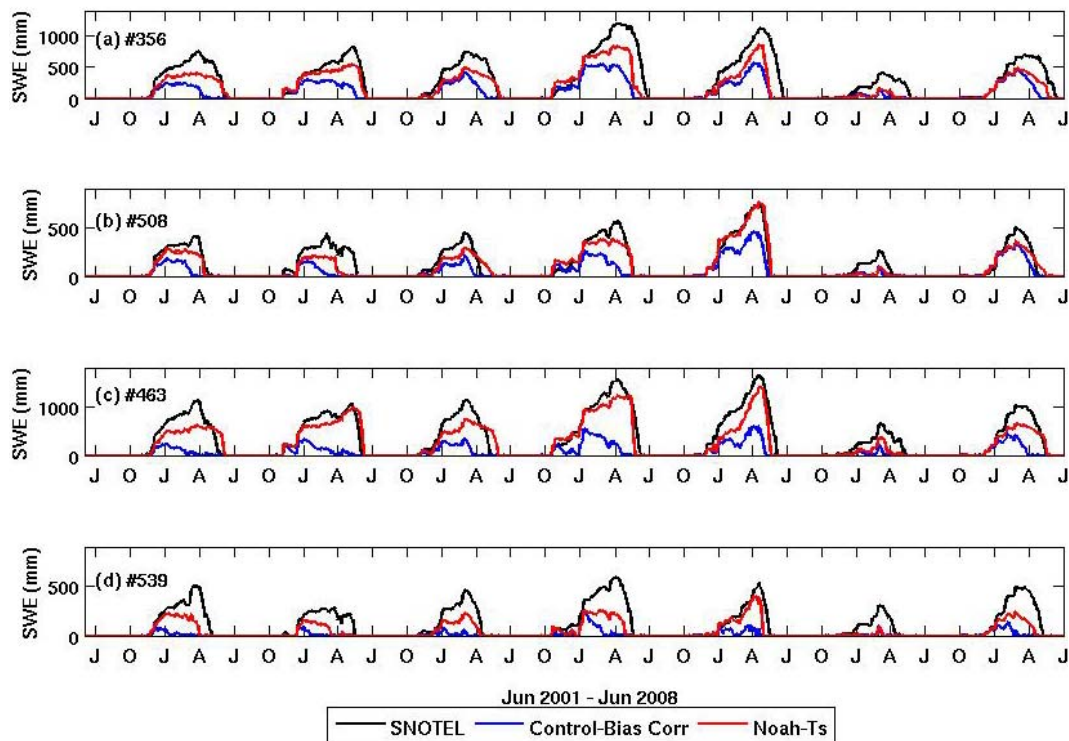


**Fig. 4.** SWE from modified model run Noah- $T_s$  (red line) is compared with observations and control run, control-bias-corr, after precipitation bias correction (blue line) at **(a)** #356, **(b)** #508, **(c)** #463, and **(d)** #539.

[Title Page](#)
[Abstract](#)
[Introduction](#)
[Conclusions](#)
[References](#)
[Tables](#)
[Figures](#)
[⏪](#)
[⏩](#)
[◀](#)
[▶](#)
[Back](#)
[Close](#)
[Full Screen / Esc](#)
[Printer-friendly Version](#)
[Interactive Discussion](#)



## Evaluating the UEB snow model in the Noah Land-Surface Model

R. Sultana et al.

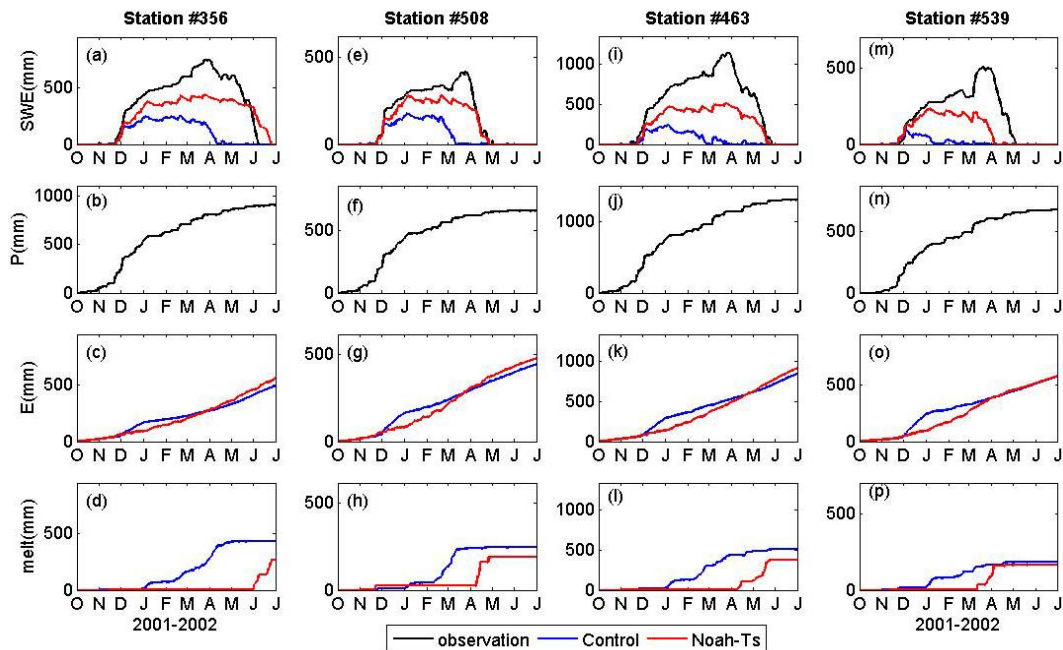


**Fig. 6.** Components of water balance on the snow surface are shown at the four SNOTEL stations for the snow season of 2001–2002. In (a), (e), (i), and (m), the snow-water equivalents simulated by the control and modified models are compared with observed SWE at #356, #508, #463, and #539 in CA, respectively. In (b), (f), (j), and (n) the accumulated precipitation at #356, #508, #463, and #539, respectively, are shown. Accumulated sublimation and snowmelt between the control and modified models are compared and shown in the third and fourth rows, respectively.

[Title Page](#)
[Abstract](#)
[Introduction](#)
[Conclusions](#)
[References](#)
[Tables](#)
[Figures](#)
[Back](#)
[Close](#)
[Full Screen / Esc](#)
[Printer-friendly Version](#)
[Interactive Discussion](#)

## Evaluating the UEB snow model in the Noah Land-Surface Model

R. Sultana et al.

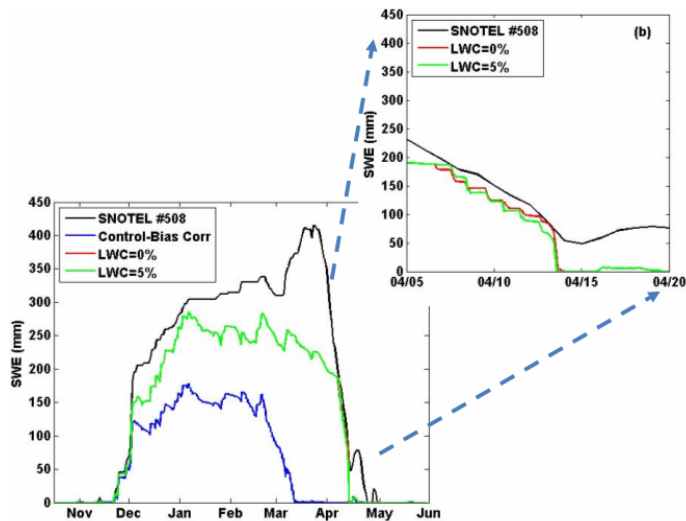


**Fig. 7.** Modified Noah LSM is simulated with 0% liquid-water content (LWC) – red line in (a) – and 5% liquid-water content – green line in (a). The results are compared with the simulated SWE from the control-bias corrected Noah LSM and ground observations at SNOTEL Station #508. The inset shows the effect of varying LWC in the modified model for 15 days in April.

[Title Page](#)[Abstract](#)[Introduction](#)[Conclusions](#)[References](#)[Tables](#)[Figures](#)[⏪](#)[⏩](#)[◀](#)[▶](#)[Back](#)[Close](#)[Full Screen / Esc](#)[Printer-friendly Version](#)[Interactive Discussion](#)

## Evaluating the UEB snow model in the Noah Land-Surface Model

R. Sultana et al.

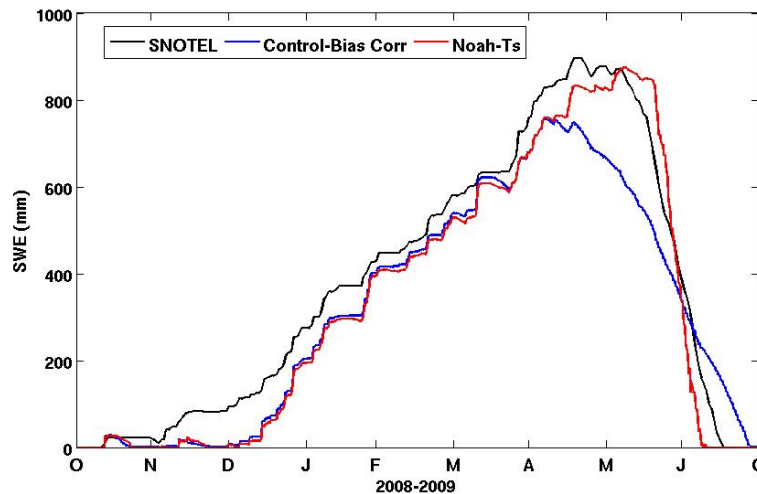


**Fig. 8.** Snow water equivalent simulated by the control and modified models are compared with observed SWE at SNOTEL Station #1098 in Utah.

[Title Page](#)[Abstract](#)[Introduction](#)[Conclusions](#)[References](#)[Tables](#)[Figures](#)[⏪](#)[⏩](#)[◀](#)[▶](#)[Back](#)[Close](#)[Full Screen / Esc](#)[Printer-friendly Version](#)[Interactive Discussion](#)

## Evaluating the UEB snow model in the Noah Land-Surface Model

R. Sultana et al.

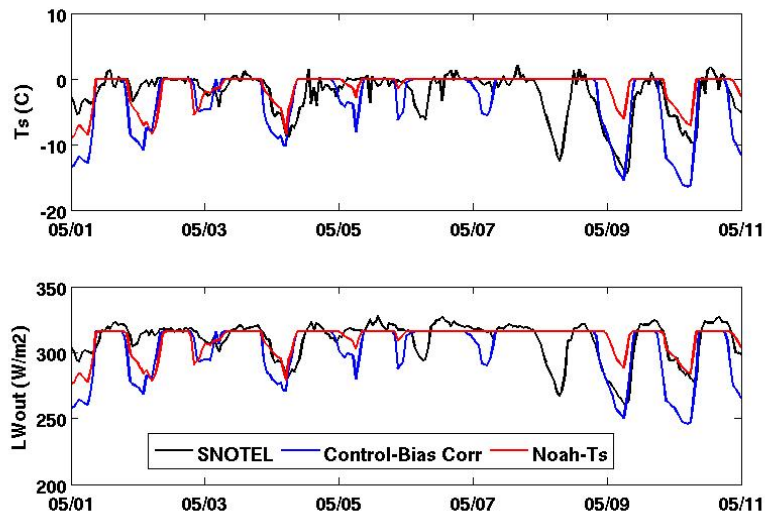


**Fig. 9.** (a) Snow-surface temperature and (b) long-wave radiation  $Q_{l,out}$  from the control and modified models are evaluated against recorded snow temperature and outgoing long-wave radiation data at the TWDEF site near SNOTEL station #1098 during the 10 day period in May 2009.

[Title Page](#)[Abstract](#)[Introduction](#)[Conclusions](#)[References](#)[Tables](#)[Figures](#)[⏪](#)[⏩](#)[◀](#)[▶](#)[Back](#)[Close](#)[Full Screen / Esc](#)[Printer-friendly Version](#)[Interactive Discussion](#)

## Evaluating the UEB snow model in the Noah Land-Surface Model

R. Sultana et al.

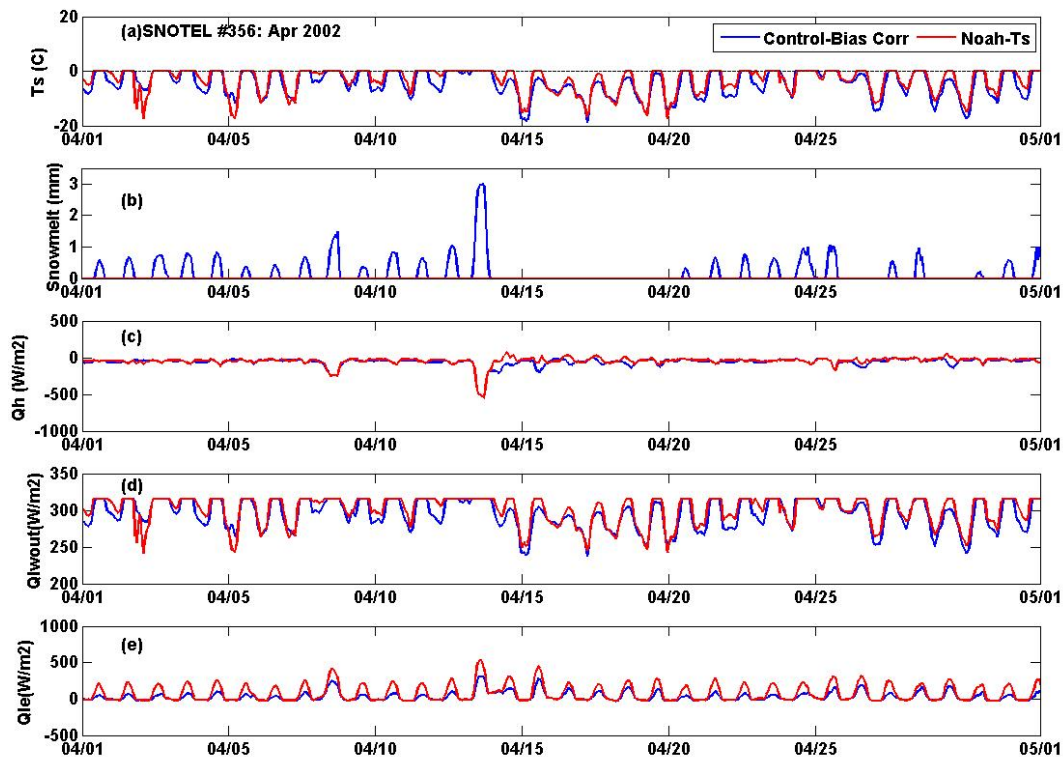


**Fig. 10.** Simulated surface temperature and energy on the snow surface is compared between control and Noah- $T_s$  models at SNOTEL station #356 during the month of April 2002.

[Title Page](#)[Abstract](#)[Introduction](#)[Conclusions](#)[References](#)[Tables](#)[Figures](#)[⏪](#)[⏩](#)[◀](#)[▶](#)[Back](#)[Close](#)[Full Screen / Esc](#)[Printer-friendly Version](#)[Interactive Discussion](#)

## Evaluating the UEB snow model in the Noah Land-Surface Model

R. Sultana et al.

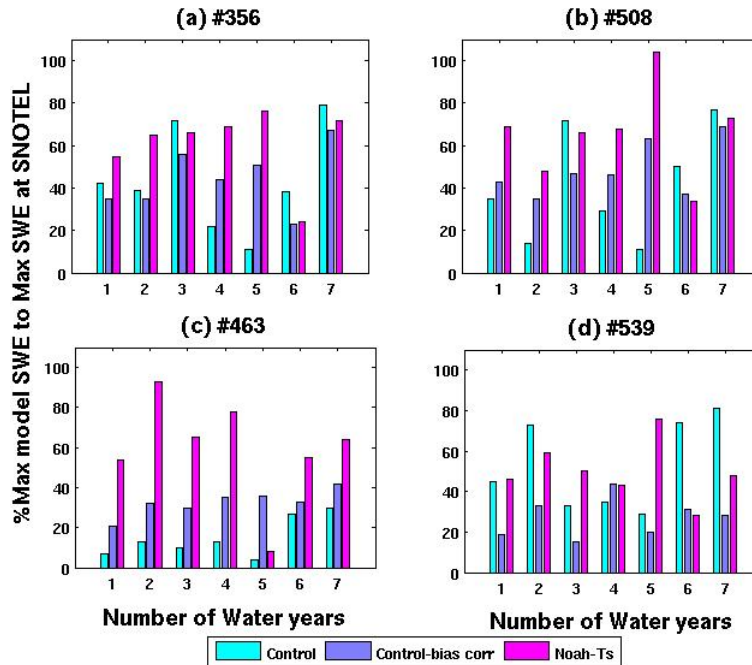


**Fig. 11.** Simulated maximum SWE as a percentage of observed maximum SWE for seven years at four CA SNOTEL stations **(a)** #365, **(b)** #508, **(c)** #463, and **(d)** #539.

[Title Page](#) | [Abstract](#) | [Introduction](#) | [Conclusions](#) | [References](#) | [Tables](#) | [Figures](#)

[⏪](#) | [⏩](#) | [⏴](#) | [⏵](#)

[Back](#) | [Close](#)

[Full Screen / Esc](#)

[Printer-friendly Version](#)

[Interactive Discussion](#)



## Evaluating the UEB snow model in the Noah Land-Surface Model

R. Sultana et al.

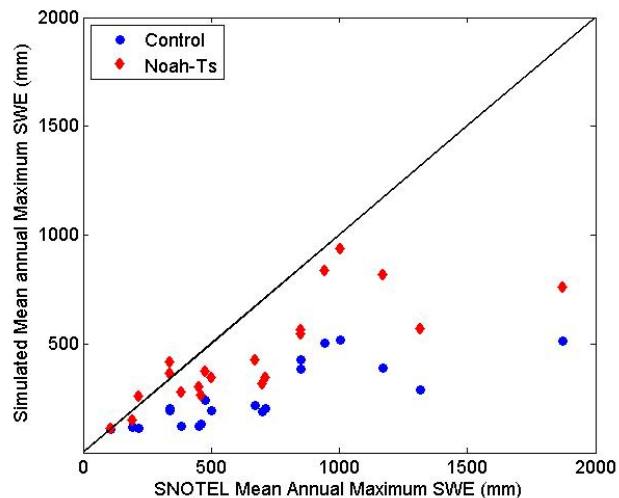


**Fig. 12.** Comparison of mean (of 7 yr of the study period) annual maximum SWE between model simulations and SNOTEL measurements (mm).

[Title Page](#)[Abstract](#)[Introduction](#)[Conclusions](#)[References](#)[Tables](#)[Figures](#)[⏪](#)[⏩](#)[◀](#)[▶](#)[Back](#)[Close](#)[Full Screen / Esc](#)[Printer-friendly Version](#)[Interactive Discussion](#)

Evaluating the UEB snow model in the Noah Land-Surface Model

R. Sultana et al.

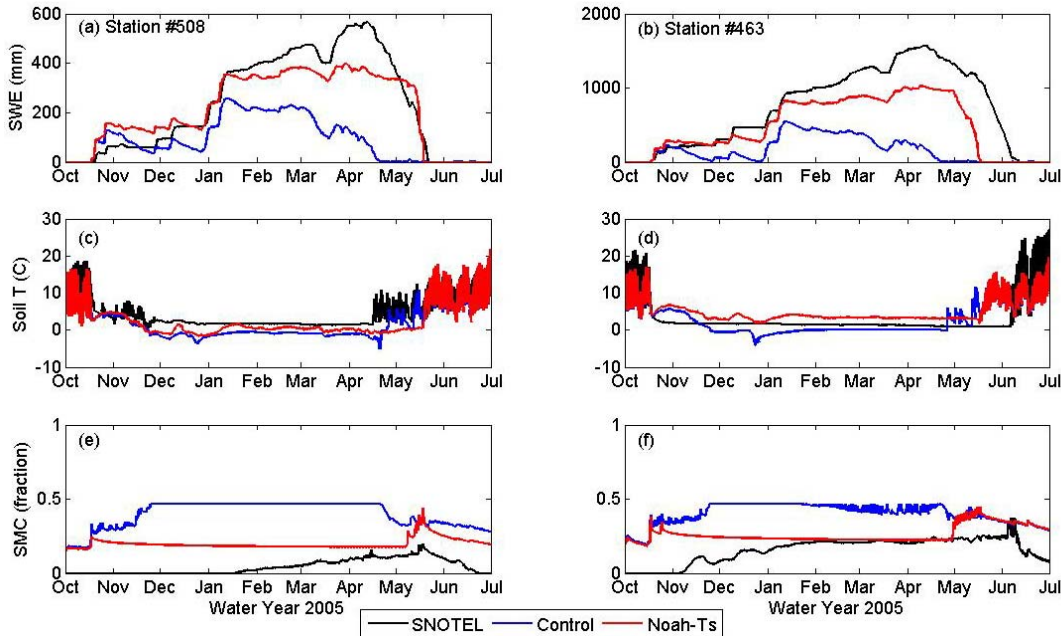


**Fig. 13.** Soil temperature (c, d) and soil-moisture content (e, f) of the first soil layer in the model is compared with observed soil temperature at Station #508 and Station #463 for water year 2005, respectively.

Title Page

Abstract Introduction

Conclusions References

Tables Figures

⏪ ⏩

⏴ ⏵

Back Close

Full Screen / Esc

Printer-friendly Version

Interactive Discussion

